$^{19}F/^{23}Na$ Double Resonance MAS NMR Study of Oxygen/Fluorine Ordering in the Oxyfluoride $Na_5W_3O_9F_5$

Lin-Shu Du,† Ago Samoson,‡ Tiit Tuherm,‡ and Clare P. Grey*,†

Department of Chemistry, State University of New York at Stony Brook, Stony Brook, New York 11794-3400, and National Institute of Chemical Physics and Biophysics, EE-0026 Tallinn, Estonia

Received May 2, 2000. Revised Manuscript Received August 22, 2000

Three resonances corresponding to the three crystallographically distinct fluorine sites were resolved in the high-resolution ^{19}F MAS spectrum of chiolite ($Na_5Al_3F_{14}$) collected at a field strength of 19.6 T and at a spinning speed of 40 kHz. In contrast, only one broad resonance is observed in the ^{19}F MAS NMR spectrum of the isostructural compound $Na_5W_3O_9F_5$. Thus, a combination of ^{19}F MAS, $^{19}F \rightarrow {}^{23}Na$ CP, and $^{23}Na \rightarrow {}^{19}F$ HETCOR NMR experiments was required to resolve the resonances from the different local environments in this compound. Fluorine was shown to preferentially occupy two of the three anion sites.

Introduction

Solid-state NMR spectroscopy is a potential method for studying ordering in disordered systems such as glasses and disordered ceramics.[1−4] For example, we have used ^{125}Te MAS NMR to distinguish between disorder originating from stacking faults (one-dimensional disorder) or from substitution (three-dimensional disorder), in a series of layered tellurates.[5,6] We have also applied fast ^{19}F MAS NMR to study disorder in crystalline fluorides, systems in which the disorder of the fluorine ions plays an important role in controlling ionic conductivity.[7,8] Oxygen/fluorine ordering is very difficult to determine from both X-ray and neutron diffraction experiments, due to the similar scattering factors of O and F in both experiments. In many instances, where anion ordering has been proposed, this has been deduced from bond-strength−bond-length calculations,[9,10] from Raman spectroscopy,[11] or from Madelung calculations.[12] In a previous paper we showed that the different local environments for fluorine could be resolved in a series of molybdenum, tungsten, and niobium oxyfluorides, allowing the extent of O/F ordering to be determined.[13] In this paper, very fast ^{19}F MAS NMR is used to study O/F ordering in a tungsten oxyfluoride, $Na_5W_3O_9F_5$.

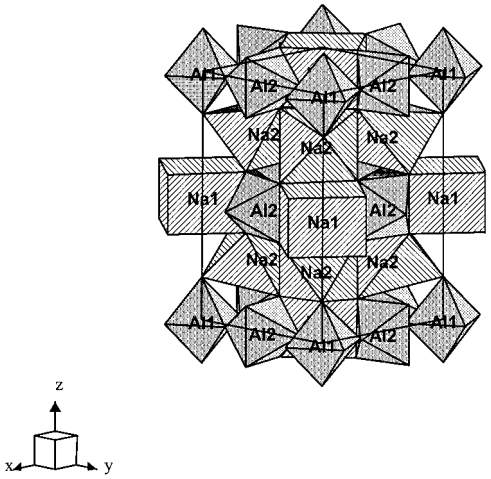

Figure 1. The structure of chiolite $Na_5Al_3F_{14}$.

$Na_5W_3O_9F_5$, which adopts the chiolite structure,[14] is a ferroelectric−ferroelastic oxyfluoride with a high F/O value.[15] The mineral chiolite, $Na_5Al_3F_{14}$, consists of alternating layers of corner-sharing AlF_6 octahedra and edge-sharing NaF_6 octahedra (Figure 1).[16,17] The Al layer contains Al1 atoms (see Figure 1) linked by bridging fluorine atoms to four other Al octahedra (Al2 in Figure 1). The ratio of Al1 to Al2 atoms is 1:2. An 8-fold cubically coordinated Na site, labeled Na1 in

* To whom correspondence should be addressed. Phone: 631-632-9548. FAX: 631-632-5731. E-mail:cgrey@notes.cc.sunysb.edu
† State University of New York at Stony Brook
‡ National Institute of Chemical Physics and Biophysics

(1) Fitzgerald, J. J.; DePaul, S. M. *ACS Symp. Ser.* **1999**, *717*, 2−133.
(2) Smith, M. E. *ACS Symp. Ser.* **1999**, *717*, 377−404.
(3) van Wuellen, L.; Gee, B.; Zuechner, L.; Bertmer, M.; Eckert, H. *Ber. Bunsen-Ges.* **1996**, *100*, 1539−1549.
(4) Stebbins, J. F. *Rev. Mineral.* **1995**, *32*, 191−246.
(5) Woodward, P. M.; Sleight, A. W.; Du, L.-S.; Grey, C. P. *J. Solid State Chem.* **1999**, *147*, 99−116.
(6) Woodward, P. M.; Sleight, A. W.; Du, L.-S.; Grey, C. P. *Mater. Res. Soc. Symp. Proc.* **1999**, *547*, 233−238.
(7) Wang, F.; Grey, C. P. *Chem. Mater.* **1997**, *9*, 1068−1070.
(8) Wang, F.; Grey, C. P. *Chem. Mater.* **1998**, *10*, 3081−3091.
(9) Torardi, C. C.; Brixner, L. H. *Mater. Res. Bull.* **1985**, *20*, 137−145.
(10) Brown, I. D.; Shannon, R. D. *Acta Crystallogr.* **1973**, *A29*, 266−282.
(11) Beattie, I. R.; Gilson, T. R. *J. Chem. Soc.* **1969**, *(A)*, 2322−2327.
(12) Wingefeld, G.; Hoppe, R. *Z. Anorg. Allg. Chem.* **1984**, *518*, 149−160.
(13) Du, L.-S.; Wang, F.; Grey, C. P. *J. Solid St. Chem.* **1998**, *140*, 285−294.
(14) Doumerc, J. P.; Elaatmani, M.; Ravez, J.; Pouchard, M.; Hagenmuller, P. *Solid State Commun.* **1979**, *32*, 111−113.
(15) Ravez, J. *J. Phys. III* **1997**, *7*, 1129−1144.
(16) Brosset, C. *Z. Anorg. Allg. Chem.* **1938**, *238*, 208.
(17) Jacoboni, C.; Leble, A.; Rousseau, J. J. *J. Solid State Chem.* **1981**, *36*, 297−304.

10.1021/cm000355h CCC: $19.00
Published on Web 11/04/2000

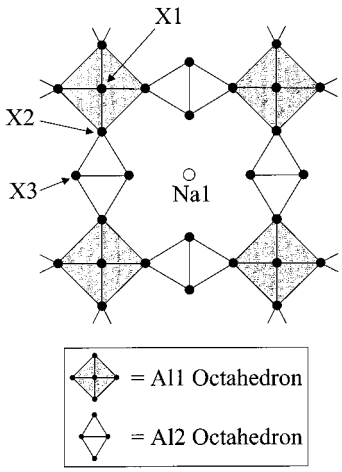

Figure 2. The anion sites, labeled X1, X2 and X3, in the ideal chiolite layer, viewed along the *z* axis.

Figure 1, is located within the Al layer and is bound to four $Al2F_6$ octahedra. The ratio of the cubically coordinated Na1 site to the octahedrally coordinated Na site in the Na layer (Na2) is 1:4. A detailed refinement of the $Na_5W_3O_9F_5$ structure has been performed at different temperatures by Abrahams et al. in order to understand the ferroelectric−ferroelastic properties of this material.[18] Oxygen/fluorine ordering in $Na_5W_3O_9F_5$ has been studied by Raman scattering.[19] On the basis of these Raman results, a model for the O/F ordering was proposed, where the bridging anion site, X2, is fully occupied by oxygen (Figure 2), while the other two sites, X1 and X3, are half-occupied by F and half-occupied by O, resulting in trans O−W1−F, cis O−W2−O, and cis F−W2−F linkages, where W1 and W2 correspond to the Al1 and Al2 sites in chiolite, respectively.

^{27}Al, ^{23}Na, and ^{19}F solid-state NMR have been used to study the sodium fluoroaluminates, chiolite, and cryolite (Na_3AlF_6).[20−22] The ^{23}Na MAS spectra of chiolite were originally reported by Stebbins et al.[20] Two overlapping resonances were observed at room temperature with intensity ratios 1:2. Values for the quadrupolar coupling constants (QCCs), asymmetry parameters (η), and chemical shifts (δ_{iso}) of QCC = 3.2 MHz, $\eta = 0.15$, and $\delta_{iso} = -6$ ppm, for the six-coordinated site, and QCC = 1.5 MHz, $\eta = 0$, and $\delta_{iso} = -21$ ppm, for the eight-coordinated Na site, were extracted. A shift in the ^{23}Na resonance to lower frequency for both chiolite and cryolite, as the sodium coordination number increased, was noted.[21] The chemical shifts of the ^{27}Al octahedra were found to be controlled by the number of bridging Al−F−Al atoms, a shift to lower frequency being observed as the number of bridging fluorine atoms increased. The variable-temperature ^{27}Al, ^{23}Na, and ^{19}F static NMR spectra were also collected in order to probe the cation diffusion and the nature and causes of the phase transitions in both cryolite and chiolite.[22] Sodium mobility in chiolite was shown to be limited to within the layers of edge-sharing NaF_6 octahedra (Na2 in Figure 1), and no exchange between the Na1 and Na2 was observed. No significant change of the ^{19}F spectra was seen, up to 150 °C, indicating the lack of any oscillatory motions of the AlF_6 octahedra in chiolite in this temperature range.

In this paper, both chiolite and the isostructural oxyfluoride are studied. A series of NMR experiments including ^{19}F and ^{23}Na MAS, $^{23}Na \rightarrow {}^{19}F$ CP, and $^{19}F \rightarrow {}^{23}Na$ HETCOR are used to first assign all three fluorine resonances in chiolite to their respective crystallographic sites. Results from the isostructural compound are then used to help explain the $^{23}Na/^{19}F$ spectra of $Na_5W_3O_9F_5$ and to study the O/F ordering in this compound.

Experimental Section

Sample Preparation. $Na_5W_3O_9F_5$ was made from a stoichiometric mixture of NaF and WO_3, which was ground in air and pressed into a 13 mm pellet and placed into a copper tube. The tube was crimped and sealed with silver solder. The tube was heated at 700 °C for 4 days and then annealed at 200 °C for 2 days. The product was characterized with powder X-ray diffraction (XRD); the X-ray powder pattern was compared to that reported in JCPDS, confirming the presence of only one phase ($Na_5W_3O_9F_5$). $Na_5Al_3F_{14}$ was obtained from Dr. N. Dando (ALCOA).

NMR Measurements. Fluorine-19 NMR spectra were obtained at a field strength of 8.5 T with a wide-bore Chemagnetics CMX-360 and at a field strength of 19.6 T with a narrow-bore Bruker AMX-833 at operating frequencies of 338.7 and 783.8 MHz, respectively. Sodium-23 MAS NMR spectra were obtained at a field strength of 8.5 T with a CMX-360 spectrometer at an operating frequency of 95.23 MHz. Fluorine-19 and sodium-23 chemical shifts are expressed in ppm relative to $CFCl_3$ and aqueous NaCl (at 0 ppm). A Chemagnetics pencil probe with a reduced ^{19}F background signal was used at 8.5 T. This probe is equipped with a high-speed MAS stator and 3.2 mm rotors that are capable of reaching spinning speeds of 24 kHz. Typically, spectra were acquired with $\pi/2$ pulses of 2 μs and recycle delays of 10 s for ^{19}F and with pulse lengths of less than $\pi/16$ (~0.2 μs) and recycle delays of 3 s for ^{23}Na. Each spectrum required approximately 40−200 acquisitions. An ultrafast MAS probe that was designed and built at the National Institute of Chemical Physics and Biophysics (Tallinn) and has 2.0 mm rotors that can reach spinning speeds of 50 kHz was used for the acquisition of ^{19}F MAS spectra at 19.6 T. The $^{19}F \rightarrow {}^{23}Na$ and $^{23}Na \rightarrow {}^{19}F$ CP MAS and $^{19}F \rightarrow {}^{23}Na$ HETCOR experiments were performed at 8.5 T at spinning speeds of 20 kHz. In these experiments, rf field strengths of ~5 and ~30 kHz, determined on the actual sample, were used for ^{23}Na and ^{19}F, respectively, to match the optimal Hartmann−Hahn condition for quadrupolar nuclei with nonzero quadrupole coupling constants:[23,24] $\omega_{1I} = (S + {}^1/_2)\omega_{1S} + n\omega_r$; $n = \pm 1$, where ω_{1I} and ω_{1S} are the rf field strengths for spin I (^{19}F) and spin S (^{23}Na), respectively, and ω_r is the spinning frequency. These CP conditions correspond to the sudden-passage regime, where adiabatic passages between the eigenstates of quadrupolar nuclei spin systems do not occur.[23,24] A contact time of 500 μs was used for the CP experiments, which corresponds to an optimal ^{19}F to ^{23}Na CP efficiency for directly coordinated Na−F atoms.[25] The $^{19}F \rightarrow {}^{23}Na$ HETCOR experiments were performed with the same CP conditions as used for the CP experiments, except that a shorter contact time of only 50 μs (which corresponds to one rotor period) was used in order to probe the shortest Na−F

(18) Abrahams, S. C.; Marsh, P.; Ravez, J. *Acta Crystallogr.* **1989**, *B45*, 364−370.
(19) Couzi, M.; Rocquet, P.; Chaminade, J. P.; Ravez, J. *Ferroelectrics* **1988**, *80*, 113−116.
(20) Stebbins, J. F.; Farnan, I.; Dando, N.; Tzeng, S.-Y. *J. Am. Ceram. Soc.* **1992**, *75*, 3001−3006.
(21) Dirken, P. J.; Jansen, J. B. H.; Schuiling, R. D. *Am. Miner.* **1992**, *77*, 718−724.
(22) Spearing, D. R.; Stebbins, J. F.; Farnan, I. *Phys. Chem. Miner.* **1994**, *21*, 373−386.
(23) Vega, A. J. *J. Magn. Reson.* **1992**, *96*, 50−68.
(24) Vega, A. J. *J. Solid State Nucl. Magn. Reson.* **1992**, *1*, 17−32.
(25) Lim, K. H.; Grey, C. P. *Chem. Commun.* **1998**, *20*, 2257−2258.

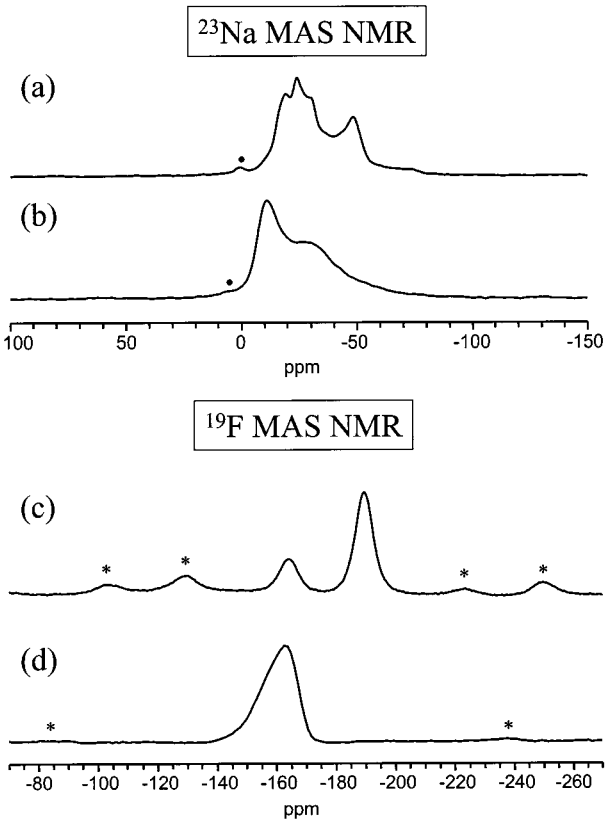

Figure 3. ^{23}Na MAS spectra of (a) $Na_5Al_3F_{14}$ and (b) $Na_5W_3O_9F_5$, and ^{19}F MAS spectra of (c) $Na_5Al_3F_{14}$ and (d) $Na_5W_3O_9F_5$ collected at a field strength of 8.5 T and a spinning speed (ν_r) of 20 kHz. The asterisks denote spinning sidebands; small impurity peaks not detected by XRD (labeled as ●) are seen at ca. 0 and − 5 ppm, in a and b, respectively.

distances. The 2-D data were collected using the time proportional phase increment method (TPPI), to obtain phase sensitive detection in the t_1 dimension.

Results and Discussion

^{23}Na MAS NMR. The ^{23}Na MAS spectra of $Na_5Al_3F_{14}$ and $Na_5W_3O_9F_5$, collected at 8.5 T and at spinning speeds of 20 kHz, are shown in parts a and b of Figure 3. Two distinct resonances with line shapes broadened by the second-order quadrupolar interaction were observed in each spectrum. This is consistent with the crystallographic results where two type of sodium sites, one coordinated to six anion sites (labeled Na2) and the other coordinated to eight anion sites (Na1) were found. The quadrupolar and chemical shift parameters obtained by simulating the ^{23}Na MAS spectrum of $Na_5Al_3F_{14}$ are consistent with those reported by Stebbins et al.[20] ($\delta_{iso} = -6$ and -21 ppm, QCC = 3.2 and 1.5 MHz, and $\eta = 0.15$ and 0, for Na1 and Na2, respectively). Simulations of the spectrum of $Na_5W_3O_9F_5$ show that there are significant distributions in the chemical shifts and quadrupolar parameters for both Na sites. Estimated parameters for Na1 and Na2 are $\delta_{iso} = -6.5$ and -16 ppm, QCC = 1.3 and 2.0 MHz, and $\eta = 0$ and 0.5, respectively. Since the ratio of the multiplicities of Na1 to Na2 is approximately 1:4, the broad, more intense, resonance is assigned to Na2, while the sharp, less intense, resonance is assigned to Na1.

^{19}F MAS NMR. The ^{19}F MAS spectra of chiolite and the oxyfluoride, collected at 8.5 T and at spinning speeds of 20 kHz, are shown in parts c and d of Figure 3. There are two resonances, −163.8 and −189.9 ppm, in the spectrum of $Na_5Al_3F_{14}$ with an intensity ratio of 2:5. A broad asymmetric fluorine resonance ranging from −135 to −180 ppm was observed for $Na_5W_3O_9F_5$. There are three crystallographic fluorine sites in $Na_5Al_3F_{14}$,[16,17] named F1, F2, and F3, as shown in Figures 2 and 4 a−c, with multiplicities of 4, 8, and 16, respectively. F1 is coordinated to one Al1 and four Na2 atoms, F2 is bonded to two Al sites (Al1 and Al2) and two more distant Na2, while F3 is coordinated with one Al2, two Na2, and one Na1 atom. Thus, the F2 site possesses a very different local environment than the other fluorine sites, due to the two adjacent Al atoms. A significant chemical shift difference between F2 and the other fluorine sites (F1 and F3) is therefore predicted. On the basis of these chemical shift arguments, and the intensities of the resonances in Figure 3c, we assign the resonance at −163.8 ppm to the F2 site. The F1 and F3 resonances clearly have very similar chemical shifts and cannot be resolved at the field strength of 8.5 T.

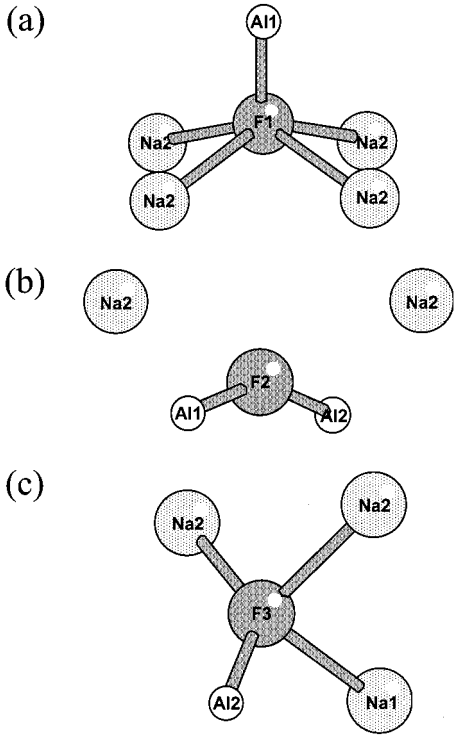

Figure 4. Local environments of the three crystallographically distinct fluorine sites, (a) F1, (b) F2, and (c) F3, in chiolite. Na−F bonds of <2.7 Å are shown.

A dramatic (∼3-fold) improvement in resolution is obtained at a high magnetic field strength (19.6 T) and a very fast spinning speed (40 kHz) (see dotted and solid lines in Figure 5 a). Thus, the broadening of the line width in the ^{19}F MAS NMR resonances at lower fields and spinning speeds is mainly due to the ^{19}F homonuclear dipolar interaction. This interaction is significantly reduced at higher fields and spinning speeds. The increase in field increases the chemical shift difference (in units of hertz) between resonances, decreasing the spectral overlap between the different resonances, thus making it easier to average the dipolar coupling between different resonances. Three resonances may now be clearly resolved in the spectrum of $Na_5Al_3F_{14}$ at −165.0, −189.5, and −191.4 ppm with intensity ratios of 2:4:1,

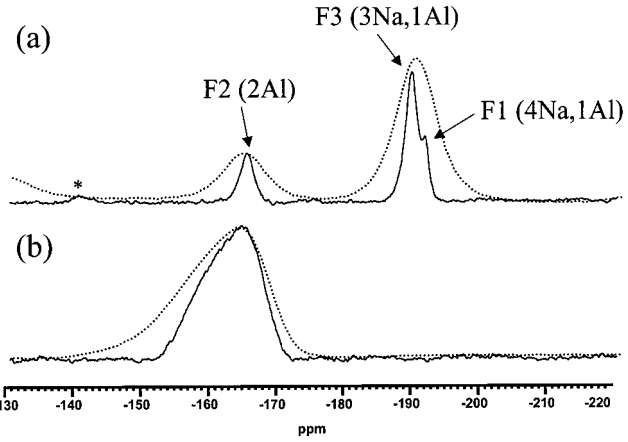

Figure 5. The ^{19}F MAS spectra of (a) $Na_5Al_3F_{14}$ and (b) $Na_5W_3O_9F_5$, collected at 19.6 T for $\nu_r = 40$ kHz (solid lines). The data collected at 8.5 T and $\nu_r = 20$ kHz are also shown (dotted lines) for comparison. The asterisk denotes a spinning sideband.

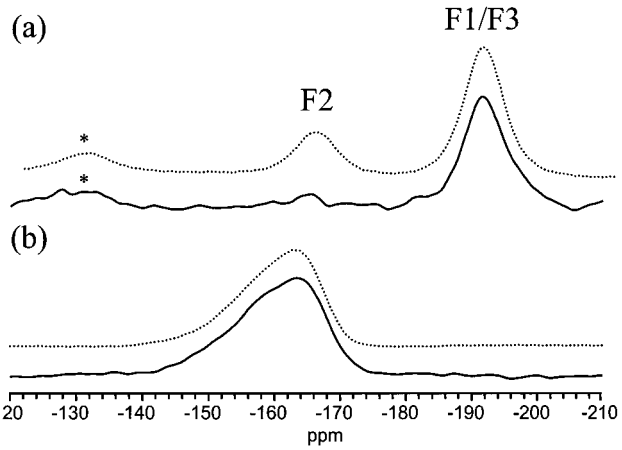

Figure 6. The $^{23}Na \rightarrow {}^{19}F$ CP MAS spectra of (a) $Na_5Al_3F_{14}$ and (b) $Na_5W_3O_9F_5$, collected at a field strength of 8.5 T and $\nu_r = 20$ kHz (solid lines). The ^{19}F carrier frequency was placed in the center between the two groups of resonances for $Na_5Al_3F_{14}$. The ^{19}F MAS data are shown as dotted lines for comparison.

which can be readily assigned to the F2, F3, and F1 sites, respectively, on the basis of their multiplicities.

The high-field spectrum of $Na_5W_3O_9F_5$ is shown in Figure 5b as a solid line. Although the line width at 19.6 T is narrower than that at 8.4 T (dotted line in Figure 5b), the resonance is still extremely asymmetric. Clearly, a major contribution to the residual line broadening seen in this more fluorine-dilute sample, at high fields and spinning speeds, must arise from local disorder and not from residual homonuclear dipolar coupling.

An assignment of the ^{19}F spectrum of $Na_5W_3O_9F_5$ is essential in order to establish the nature of the oxygen/fluorine ordering. Due to the lower symmetry space group of $Na_5W_3O_9F_5$ (*I*2) in comparison to that of $Na_5Al_3F_{14}$ (*Pr*/*mnc*), there are eight different crystallographic anion sites in $Na_5W_3O_9F_5$ instead of three.[18] However, these anions can be grouped to three types of anions, X1, X2, and X3, on the basis of their coordination environments, where the same labeling scheme for the anion sites, as is used for chiolite, has been employed. Thus, the prototype chiolite structure will be used for the following discussion of O/F ordering. There are 14 anion sites per formula unit in the high-symmetry chiolite structure (*Pr*/*mnc*), two X1, four X2, and eight X3 sites, which are occupied by nine oxygen atoms and five fluorine atoms. The oxygen anions will show a tendency to order on the site coordinated to the largest number of higher valent cations (W^{6+}), (i.e., X2), as was proposed previously.[13] Thus is it appears reasonable to assume that all X2 sites are occupied by four out of the nine oxygen atoms. There are then three major possibilities for the anion distributions in the remaining two sites: (1) preferential occupation of O in X1, (2) preferential occupation of O in X3, and (3) random substitution of O on both sites.

Each of these distributions results in different numbers of fluorine atoms occupying the X1 and X3 sites and thus very different F1:F3 intensity ratios of 0:5, 2:3, and 1:4 for models 1, 2, and 3, respectively, where F1 and F3 denote the fluorine atoms in X1 and X3, respectively. Unfortunately the two sites cannot be resolved at both high and low fields. Simulations of the asymmetric line shapes by using two resonances with relative intensities given by the three models were attempted, and the best fit to the experimental spectrum was obtained with intensity ratios of 3:2 and chemical shifts of ca. −158 and −164 ppm, consistent with model 2. The intensity ratios and chemical shifts extracted from these simulations are not, however, unambiguous, and thus, $^{23}Na \rightarrow {}^{19}F$ CP and $^{19}F \rightarrow {}^{23}Na$ HETCOR experiments were performed to explore the connectivity between Na and F, to test the different models. These experiments are discussed in the following sections.

Table 1. Na−F and F−F Distances (in Å) in for the Three Fluorine Sites in $Na_5Al_3F_{14}$ to within 3 Å

F1		F2		F3	
F2 × 4	2.53	F3 × 2	2.51	Na2	2.27
				Na2	2.29
		F1 × 2	2.53	F3	2.49
				F2	2.51
Na2 × 4	2.63	F2 × 2	2.54	F3	2.57
				Na1	2.58
		F1 × 2	2.60	F2	2.60
		Na2 × 2	2.84		

$^{23}Na \rightarrow {}^{19}F$ CP. Parts a and b of Figure 6 show the $^{23}Na \rightarrow {}^{19}F$ CP (solid lines) and ^{19}F MAS (dotted lines) spectra of $Na_5Al_3F_{14}$ and $Na_5W_3O_9F_5$, respectively. The CP efficiencies for CP to F1 and F3 are very similar and are clearly much greater than that for F2 in $Na_5Al_3F_{14}$. From Table 1 and Figure 4, F2 is seen to be coordinated to only two sodium atoms with relatively long Na−F bond distances of 2.84 Å, resulting in the poorer CP efficiency. The $^{23}Na \rightarrow {}^{19}F$ CP efficiency for F2 is thus inferior to that for the F1 and F3 sites, where there are four and three Na atoms nearby, respectively. Note that although there is one less Na atom to within 3 Å around the F3 site than around the F1 site, the Na−F3 bond distances are shorter, clearly resulting in similar CP behavior for the two sites. In contrast, no discernible difference is seen between the ^{19}F MAS and CP line shapes for the broad asymmetric resonance in $Na_5W_3O_9F_5$ (Figure 6b). Thus, the resonance does not appear to arise from F2 sites but must arise from F1/F3 sites. Furthermore, the lack of change in the line shape suggests that the CP efficiencies of F1 and F3 sites in $Na_5W_3O_9F_5$ are also very similar, as was observed for $Na_5Al_3F_{14}$.

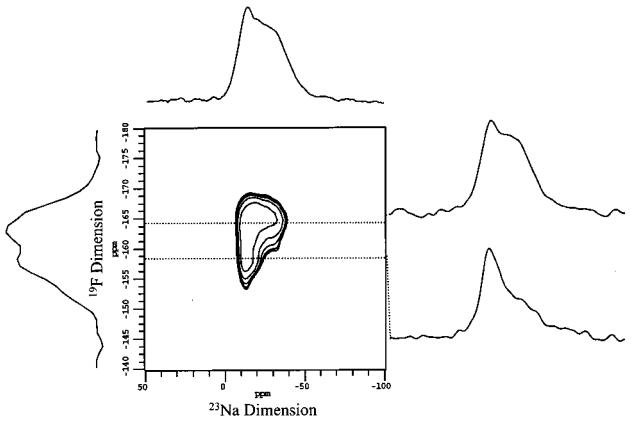

Figure 7. The $^{19}F \rightarrow {}^{23}Na$ HETCOR spectrum of $Na_5W_3O_9F_5$ depicted as a 2-D contour plot, collected at a field strength of 8.5 T and $\nu_r = 20$ kHz, with a CP contact time of 50 μs. The projection spectra for both dimensions are also displayed. The horizontal slices through the resonance frequencies at −164.3 and −157.8 ppm in the ^{19}F dimension are shown on the top and bottom, respectively, at the right-hand side of the 2D contour plot.

$^{19}F \rightarrow {}^{23}Na$ HETCOR. A $^{19}F \rightarrow {}^{23}Na$ HETCOR experiment was conducted for $Na_5W_3O_9F_5$ with a very short CP contact time (50 μs), to try to separate the two fluorine sites on the basis of any differences between their cross-polarization transfer dynamics from the two Na sites. The result is shown in Figure 7 as a contour plot with the ^{23}Na and ^{19}F frequencies displayed in the horizontal and vertical directions, respectively. Two different resonances are now resolved in the projection of the ^{19}F dimension, at −164.3 and −157.8 ppm. Slices through these two peaks show very different Na connectivity: the resonance from Na2 dominates the slice through −164.3 ppm, while the slice through −157.8 ppm contains both resonances. Returning to the F1 environment in chiolite (see Table 1/Figure 4), F1 contains only Na2 sites in its local coordination sphere and the next coordination sphere contains only one Na1 atoms at a distance 3.42 Å away from the F1 site. On the other hand, the F3 atom is coordinated to two Na2 sites and one Na1 site. Thus, the resonances at −157.8 and −164.3 ppm are assigned to F3 and F1 sites, respectively.

The ^{19}F 1D MAS spectrum was then simulated using the chemical shift positions obtained from the ^{19}F dimension of the HETCOR spectrum (Figure 7), yielding intensity ratios of F3:F1 of approximately 3(±0.2): 2(±0.2). This is consistent with a preference of oxygen for the X3 site (over the X1 site). Although there may clearly be an error associated with the deconvolution shown in Figure 8, a number of points can be made: the observation of two resonances with very different cross-polarization behavior rules out model 1, where no F1 intensity is predicted. Model 3 (i.e., random ordering on the F1/F4) predicts a F3:F1 intensity ratio of 4:1, which is also not consistent with the ^{19}F line shape. Thus, only a model where there is at least some preference of O for the X3 sites can provide a satisfactory fit to the experimental data.

Discussion of O/F Ordering in $Na_5W_3O_9F_5$. O/F ordering can be estimated by bond-length−bond-strength calculations.[10] The sums of the bond strengths (valences) for each anion site were calculated twice, first by assuming that all the anion sites were occupied by oxygen and, second, by assuming that all the anion sites contained fluorine. Anion−metal and anion−anion distances up to 5.0 Å were included in the sum, and all the different X1 sites were averaged to give a single value for the X1 environment. The process was repeated for the X2 and X3 environments. The calculated bond valences of the X1, X2, and X3 environments in $Na_5W_3O_9F_5$ are 1.348/1.064, 2.123/1.703, and 1.464/1.116, respectively, for full occupancy by either O or F. The order of the bond valences for oxygen is X2 > X3 > X1. Therefore, the O^{2-} oxygen anions should prefer to order in the X2 site, the remainder of the oxygen anions occupying the X3 site. The deconvolution of the ^{19}F MAS spectrum yielded very different line widths (full width at half-maximum) for the two resonances at −157.8 (F3) and −164.3 ppm (F1) of 4.2 and 2.3 kHz, respectively, which should also provide information concerning the ordering. The distribution in the fluorine chemical shift is likely to result from the O/F distributions in the nearest-neighbor anion sites. Considering then the local environments around the F1 and F3 sites (Table 1), there are two X3 sites located 2.49 and 2.57 Å away from the F3 sites, but no X3 sites are within 3 Å from a F1 site. Given that the O/F disorder is found on the X3 sites, a sharper resonance is predicted for the F1 resonance, as was observed experimentally.

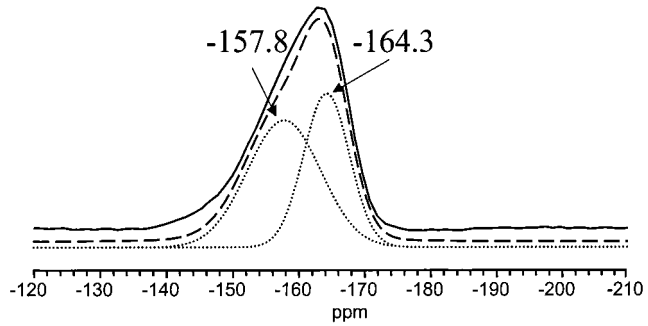

Figure 8. Deconvolution result obtained with two peaks at −157.8 and −164.3 ppm (dashed line = sum) and the ^{19}F MAS experimental spectra (solid line) of $Na_5W_3O_9F_5$ collected at 8.5 T with $\nu_r = 20$ kHz.

The O/F ordering scheme presented here differs slightly from the one proposed in the previous study.[19] In this study, the peaks in the Raman spectra were assigned to W−O oscillators with nonbridging oxygen atoms, W−O−W bridges, and W−F oscillators with nonbridging fluorine atoms. As in our O/F ordering scheme, oxygen is proposed to order in the bridging anion site, X2; however, no preference for F or O on the remaining X1 and X3 was found (i.e., model 3 in this paper). Two types of tungsten octahedra were suggested (Figure 9a): the W1 octahedron has a trans F1−W1−O arrangement, while the W2 atom is coordinated to two F3 atoms in a cis arrangement. Since the multiplicities of the W1 and W2 sites are 1 and 2, respectively, this results in a F3:F1 ratio of 4:1, as predicted by model 3. Our model is shown in Figure 9b. On the basis of the assignment of Raman spectra in the previous study and our NMR results, we propose that three types of octahedra are present. Since the X1 sites are preferentially occupied by F1, a trans F1−W1−F1 arrangement must be present. From our F3:F1 ratio of 3:2 (which indicates that three out of eight X3 sites are occupied

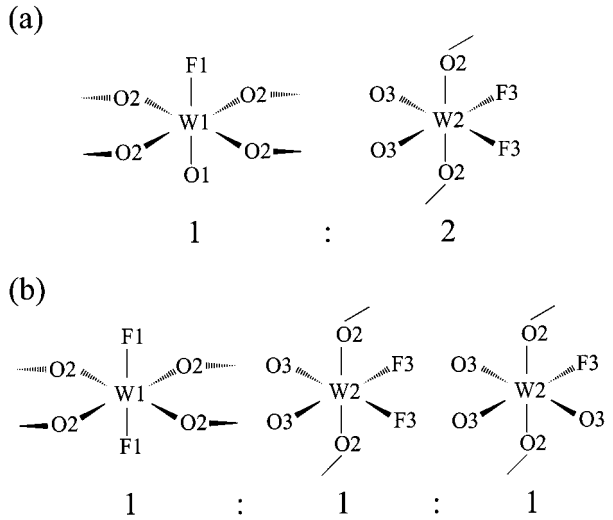

Figure 9. The different tungsten octahedra proposed on the basis of (a) a previous Raman spectroscopy study[19] and (b) from this study. The multiplicities of the different coordination environments are listed below each octahedron.

by fluorine), two types of W2 octahedra must be present, one coordinated to two F3 and one coordinated to only one F3 atom which, if the multiplicity of the W1 and W2 atoms is accounted for, results in the appropriate F3:F1 ratio. Our ordering scheme results in a slightly more uniform distribution of fluorine atoms over the two tungsten octahedra.

Conclusions

A combination of very fast ^{19}F MAS and high magnetic field strengths allowed all three fluorine sites of chiolite to be resolved for the first time. Fast MAS/high fields did not significantly improve the resolution in the ^{19}F MAS NMR of the isostructural compound $Na_5W_3O_9F_5$, indicating that the major source of broadening in the spectra of this oxyfluoride results from a distribution of chemical shifts, due to disorder on the anion sublattice. Although individual anion sites could not be resolved in this compound, double resonance two-dimensional NMR experiments were used to separate the broad ^{19}F line shape into two different components, which differed on the basis of their sodium coordination environments. Chiolite served as a model compound to test these double resonance experiments, since the different fluorine sites were well-resolved. On the basis of the assignments made from the double resonance experiments and deconvolution of the asymmetric line shape, an ordering scheme for O and F in $Na_5W_3O_9F_5$ was proposed, where oxygen orders preferentially on the W−O−W bridging positions and on the X3 site. The latter site is occupied by both F and O. The broad distribution of ^{19}F chemical shifts is then ascribed to disorder in the first anion (X3) coordination sphere. Finally, this paper shows how, despite the relatively poor resolution of the ^{19}F MAS NMR spectra due to this disorder, a series of careful double resonance experiments may still be used to separate different local environments on the basis of their different coordination environments and thus allow models for O/F ordering to be proposed.

Acknowledgment. This research was supported by a grant to C.P.G. from the National Science Foundation (DMR9901308) and through a grant to purchase the NMR spectrometer (CHE-9405436). Support of the National High Magnetic Field Laboratory (NHMFL) via the National Science Foundation Cooperative Agreement DMR-9527035 and by the State of Florida is gratefully acknowledged. Z. Gan and F. Taulelle are thanked for helpful discussions. T.T. and A.S. acknowledge support from Estonian Science Foundation.

CM000355H